Hypoxia and Hypoxia-Inducible Factor-1 Expression Enhance Osteolytic Bone Metastases of Breast Cancer

Toru Hiraga,[1,2] Shinae Kizaka-Kondoh,[3] Kiichi Hirota,[4] Masahiro Hiraoka,[3] and Toshiyuki Yoneda[1]

[1]Department of Biochemistry, Graduate School of Dentistry, Osaka University, Suita, Osaka, Japan; [2]Department of Histology and Cell Biology, Matsumoto Dental University, Shiojiri, Nagano, Japan; [3]Department of Therapeutic Radiation Oncology, Kyoto University Graduate School of Medicine; and [4]Department of Anesthesia, Kyoto University Hospital, Kyoto, Japan

Abstract

Hypoxia is a common feature of solid tumors and is associated with their malignant phenotype. The transcription factor hypoxia-inducible factor-1 (HIF-1) is a major regulator of adaptation to hypoxia and is implicated in the malignant progression of cancers. Here, we studied whether hypoxia and HIF-1 expression contribute to the development of bone metastases using a well-characterized animal model of bone metastasis in MDA-MB-231 human breast cancer cells. To study the role of hypoxia in bone metastases, we tested the effects of the fusion protein (TOP3), the oxygen-dependent degradation domain of HIF-1α fused with HIV-TAT, and procaspase-3. TOP3 selectively induced apoptosis in hypoxic tumor cells *in vitro* and significantly reduced bone metastases *in vivo*. We next examined the role of HIF-1 in bone metastases by establishing MDA-MB-231 cells overexpressing constitutively active or dominant-negative HIF-1α (MDA/CA-HIF or MDA/DN-HIF, respectively). Bone metastases of MDA/CA-HIF were significantly increased with elevated number of CD31-positive blood vessels. In contrast, bone metastases were significantly reduced in MDA/DN-HIF. Because the progression of osteolytic bone metastases is due in part to the imbalance between bone formation and bone resorption, we examined the effects of hypoxia and HIF-1 on the differentiation of osteoblasts and osteoclasts. Hypoxia and CA-HIF overexpression markedly inhibited osteoblastic differentiation, whereas hypoxia increased osteoclast-like cell formation. In conclusion, these results suggest that tumor-associated hypoxia and HIF-1 expression promote the progression of bone metastases in breast cancer. Our results also suggest that hypoxia and HIF-1 lead to the development of osteolytic bone metastases by suppressing osteoblast differentiation and promoting osteoclastogenesis. [Cancer Res 2007;67(9):4157–63]

Introduction

Hypoxia is a common feature of solid tumors, which is caused by reduced or inadequate oxygen supply (1–3). According to Vaupel et al. (4), median tumor oxygen concentration in breast cancer is ~1.3%, which is much lower than the surrounding normal tissue. Tumor hypoxia has been considered to be a potential therapeutic problem because hypoxic tumor cells are resistant to radiotherapy and chemotherapy (1–3). Furthermore, recent studies suggest that tumor hypoxia is associated with malignant biological phenotype, including enhanced invasiveness, angiogenesis, and distant metastasis (1–3).

The transcription factor hypoxia-inducible factor-1 (HIF-1), which consists of a heterodimer of HIF-1α and HIF-1β, is a major regulator for cancer cells to adapt hypoxia (2, 5). More than 60 putative direct HIF-1 target genes, including glycolytic enzymes, glucose transporter, angiogenic factors, growth factors, enzymes, and proteins involved in tumor invasiveness and metastasis, and apoptosis resistance–related proteins, have been identified (2, 5). HIF-1α possesses a unique oxygen-dependent degradation domain (ODD) that controls protein stability (2, 5, 6). Under normoxia, HIF-1α is continuously degraded by ubiquitin-proteasome pathway, which specifically targets the ODD. On the other hand, under hypoxia, HIF-1α is stabilized, dimerizes with HIF-1β, and initiates gene transcription. Clinicopathologic studies have shown that the expression level of HIF-1α in breast cancer increases as the pathologic stage elevates (7). Furthermore, increased levels of HIF-1α are associated with increased proliferation, metastasis, and poor prognosis in breast cancer patients (8–10).

Bone is one of the most common sites of metastases in breast cancer (11). Bone metastases are usually associated with devastating complications, including severe bone pain, pathologic bone fracture, hypercalcemia, and nerve compression syndromes, and causes increased morbidity and eventual mortality in breast cancer patients (11). In the present study, we studied whether hypoxia and HIF-1 contribute to the development of bone metastases using an animal model of human breast cancer. To examine the role of hypoxia in bone metastases, we used a fusion protein, which comprised of the protein transduction domain (PTD) embedded in the HIV-TAT protein, ODD, and procaspase-3 [*T*AT-PTD-*O*DD-*P*rocaspase-*3* (TOP3); refs. 2, 12]. It has been shown that HIV-TAT fusion protein can be delivered to all tissues, including brain, and used to deliver functional biomolecules *in vivo* (13). Of note, because this fusion protein contains ODD, it is degraded under the normoxic condition; however, under the hypoxic condition, the protein is stabilized and causes caspase-3–induced cell death. We previously showed that the TAT-ODD fusion protein was accumulated specifically in the hypoxic regions in tumors (12). Furthermore, TOP3 selectively killed the hypoxic cells and suppressed the tumor growth in mice (12). To examine the role of HIF-1 in bone metastases, we established MDA-MB-231 human breast cancer cells stably transfected with constitutively active or dominant-negative HIF-1α cDNA (MDA/CA-HIF or MDA/DN-HIF, respectively; refs. 14, 15). The effects of YC-1, an inhibitor of HIF-1 (16), on bone metastases of MDA-MB-231 were also studied. It is well known that the bone metastases of breast cancer are predominantly osteolytic (11); however, the mechanisms are not fully understood. To approach this, we studied the effects of hypoxia and HIF-1 on bone cells, osteoblasts, and osteoclasts, *in vitro*.

Note: Supplementary data for this article are available at Cancer Research Online (http://cancerres.aacrjournals.org/).

Requests for reprints: Toshiyuki Yoneda, Department of Biochemistry, Graduate School of Dentistry, Osaka University, 1-8 Yamadaoka, Suita, Osaka 565-0871, Japan. Phone: 81-6-6879-2887; Fax: 81-6-6879-2890; E-mail: tyoneda@dent.osaka-u.ac.jp.

doi:10.1158/0008-5472.CAN-06-2355

Materials and Methods

Reagents

Mouse monoclonal anti–HIF-1α antibody and rat monoclonal anti-CD31 antibody were purchased from BD Biosciences. Rabbit polyclonal anti-poly(ADP-ribose) polymerase (PARP) antibody and mouse monoclonal anti-FLAG antibody were from Stressgen Bioreagents Corp. and Sigma, respectively. YC-1 [3-(5′-hydroxymethyl-2′-furyl)1-benzylindazole; ref. 16] was from Alexis Corp. Recombinant human bone morphogenetic protein 2 (BMP2) was obtained as described previously (17). All other chemicals used in this study were purchased from Sigma or Wako Pure Chemical Industries, Ltd., unless otherwise described.

Cell Culture

The human breast cancer cell line MDA-MB-231 (American Type Culture Collection) was cultured in DMEM (Sigma) supplemented with 10% FCS (Asahi Glass Techno Corp.) and 100 μg/mL kanamycin sulfate (Meiji Seika Kaisha, Ltd.). C3H10T1/2 cells were purchased from RIKEN BioResource Center and cultured in α-MEM (Sigma) supplemented with 10% FCS and 100 μg/mL kanamycin sulfate. Mouse primary osteoblasts were isolated as described previously (17). All cells were maintained in a humidified atmosphere of 5% CO_2 in air. Hypoxia was achieved by incubating cells in a humidified environment at 37°C in a CO_2 incubator (ASTEC Co., Ltd.) maintained at 94% N_2, 5% CO_2, and 1% O_2.

TAT Fusion Protein

TOP3 and TAT-PTD-ODD fused to β-galactosidase (TAT-PTD-ODD-β-Gal) were prepared as previously described (12). For X-gal staining, TAT-ODD-β-Gal (1 unit of β-Gal activity/mL) was added to subconfluent MDA-MB-231 cells in 24-well plates and the cells were cultured for 24 h. X-gal staining was done as described previously (12).

Western Blot

Whole-cell lysates and nuclear extracts were prepared as described previously (17, 18). Equivalent amounts were loaded for SDS-PAGE, and immunoblotting was done (17, 18). We confirmed that equal amounts of proteins were loaded by staining the transferred membranes with Ponceau S.

Apoptosis

Subconfluent MDA-MB-231 cells in six-well plates were treated with TOP3 (15 μg/mL) for 36 h. Apoptosis in MDA-MB-231 cells were determined using a fluorescence-activated cell sorting (FACS) technique as previously described (18). The percentages of sub-G_1 nuclei in the population were determined as percentage apoptosis.

Transfection

The cDNAs encoding constitutively active (14) and dominant-negative (15) forms of HIF-1α ligated into pcDNA3 (Invitrogen) and p3XFLAG-CMV10 vector (Sigma) were transfected into MDA-MB-231 cells using FuGENE 6 Transfection Reagent (Roche Diagnostics Co.) according to the manufacturer's protocol (MDA/CA-HIF and MDA/DN-HIF). As a control, empty pcDNA3 vector was similarly transfected into MDA-MB-231 cells (MDA/EV). Colonies resistant to 1 mg/mL G418 (Sigma) were isolated and cloned.

ELISA

MDA-MB-231 cells (1×10^4) were plated in 48-well plates. When near confluence, the cells were rinsed with PBS and 250 μL of serum-free DMEM was added to each well. The conditioned medium was collected after 48 h. Concentrations of vascular endothelial growth factor (VEGF) in the conditioned medium were determined by ELISA (R&D Systems, Inc.) according to the manufacturer's instruction. Data are expressed as amount of VEGF produced (pmol/L/mL) per 10^5 cells.

Animal Experiments

Under the anesthesia with pentobarbital (0.05 mg/g body weight; Dainippon Pharmaceutical Co., Ltd.), parental MDA-MB-231, MDA/EV, MDA/CA-HIF, or MDA/DN-HIF cells (1×10^5/0.1 mL PBS) were injected into the left cardiac ventricle of nude mice (female, 4-week-old, SLC Japan Co., Ltd.) as previously described (18). TOP3 (2 or 20 mg/kg) was i.p. injected on days 14, 18, 22, and 26. YC-1 (30 mg/kg) was i.p. injected daily for 2 weeks from day 14 (16). In all experiments, mice were sacrificed at day 28. The number of mice used in each experiment was described in each figure. All animal experiments were reviewed by the Institutional Review Board of Animal Experiments in Osaka University Graduate School of Dentistry.

X-ray Analysis of Osteolytic Lesion Area

Areas of osteolytic lesions were determined on radiographs as described previously (18). Radiographs were analyzed carefully by two different individuals who had no prior knowledge of the experimental protocol. Data are shown as osteolytic lesion area (mm^2)/mouse.

Histologic and Immunohistochemical Analysis

Paraffin sections of the femora and tibiae were made as previously described (18).

Detection of hypoxia. The hypoxic regions in the bone metastases were detected using Hypoxyprobe-1 kit (Chemicon International, Inc.) according to the manufacturer's protocol. Briefly, the tumor-bearing mice were i.p. injected with pimonidazole hydrochloride (60 mg/kg) and were sacrificed 2 h later. The accumulation of pimonidazole was visualized by the immunohistochemical technique.

Immunohistochemistry. Immunohistochemical staining of HIF-1α and CD31 was done using VECTASTAIN Elite ABC kit (Vector Laboratories, Inc.) according to the manufacturer's protocol. Chromogen was developed using 3,3′-diaminobenzidine substrate kit (Vector Laboratories). The slides were counterstained with hematoxylin.

Enzyme histochemistry. Tartrate-resistant acid phosphatase (TRAP) and alkaline phosphatase activities were detected by histochemical staining technique as described previously (18, 19).

Histomorphometric Analysis

Tumor burden. Histomorphometric analysis of tumor burden in bone was done as described previously (18). Data are shown as tumor area (mm^2) / animal.

Microvessel density. CD31-positive microvessels were counted in five random fields at ×200 magnification. Data are shown as the number of CD31-positive microvessels/mm^2 tumor area.

All of the histomorphometric analyses were done extensively and carefully by two different individuals, all of whom were without knowledge of the experimental protocol.

Adenovirus

The recombinant adenovirus carrying CA-HIF-1α was constructed using Adenovirus Expression Vector Kit (TAKARA Bio, Inc.) according to the manufacturer's protocol. As a control, the adenovirus carrying enhanced green fluorescent protein (EGFP) was used. The viruses showed no proliferative activity due to a lack of E1A-E1B (20). Titers of the viruses were determined by a modified point assay (20).

Alkaline Phosphatase Staining

C3H10T1/2 cells (1×10^4 per well/48-well plate) were cultured in the presence of 100 ng/mL BMP2 for 7 days under 20% or 1% O_2. The cells were stained with a mixture of 330 μg/mL nitroblue tetrazolium, 165 μg/mL bromochoroindoylphosphate, 100 mmol/L NaCl, 5 mmol/L $MgCl_2$, and 100 mmol/L Tris (pH 9.5).

Alizarin Red Staining

Mouse primary osteoblasts (1×10^4 per well/48-well plate) were cultured in the presence of 100 ng/mL BMP2, 5 mmol/L β-glycerophosphate, and 100 μg/mL ascorbic acid for 14 days under 20% or 1% O_2. The cells were rinsed twice with PBS, fixed in 10% buffered formalin, and stained with 1% alizarin red solution for 5 min.

Reverse Transcription PCR

Total RNA was isolated using TRI Reagent (Sigma) and single-strand cDNA was synthesized using BD PowerScript Reverse Transcriptase (BD Biosciences). The primer sets used for PCR were as follows: mouse Runx2,

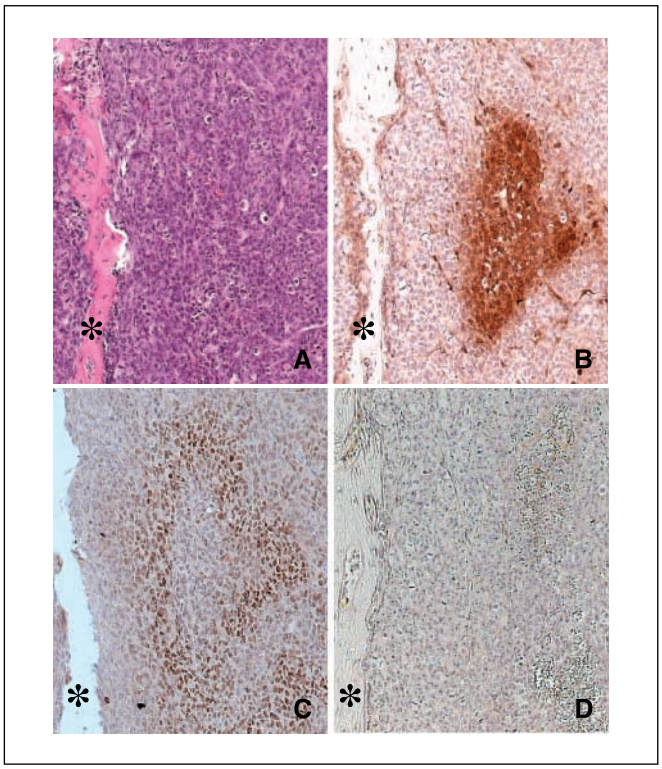

Figure 1. Hypoxia and HIF-1α expression in bone metastases of MDA-MB-231 human breast cancer cells in nude mice. Hypoxia (*B*) was determined by the accumulation of pimonidazole as described in Materials and Methods. HIF-1α expression (*C*) was determined by immunohistochemistry. (*A,* H&E staining; *D,* negative control of HIF-1α immunohistochemistry; *, bone; original magnification, ×200).

GCCGGGAATGATGAGAACTA/GGACCGTCCACTGTCACTTT; mouse osteocalcin, AAGCAGGAGGGCAATAAGGT/ACTTGCAGGGCAGAGAGAGA; mouse glyceraldehyde-3-phosphate dehydrogenase (GAPDH), TTGAAGGGTGGAGCCAAACG/ACACATTGGGGGTAGGAACACG. PCR products were separated on 2% agarose gels containing ethidium bromide and visualized under UV light. The size of the fragments was confirmed by reference to 100-bp DNA ladder. Quantification of amplified mRNA was done by densitometry assisted by the image analysis software Scion Image (Scion Corporation).

Osteoclast Differentiation *In vitro*

Spleen cells were isolated from ddY mice (male, 4-week-old, SLC Japan) and cultured in αMEM supplemented with 10% FCS, 30 ng/mL recombinant human macrophage colony-stimulating factor (M-CSF; Peprotech EC, Ltd.), and 50 ng/mL recombinant human soluble receptor activator of nuclear factor-κB ligand (sRANKL; Peprotech EC) for 6 days under normoxia or hypoxia. At the end of the culture, the cells were stained with TRAP, a marker enzyme of osteoclasts using a commercially available kit (Sigma). TRAP-positive multinucleated (three or more nuclei) cells in each well were counted under light microscope. Data are shown as number of TRAP-positive multinucleated cells per well.

Statistical Analysis

Data are expressed as the mean ± SE and were analyzed by one-way ANOVA followed by Fisher's protected least-significant differences post hoc test (StatView; SAS Institute, Inc.) for determination of differences between groups. Student's *t* test or Welch's *t* test was conducted when two groups were compared. *P* values of <0.05 were considered significant.

Results

Hypoxia in bone metastases of MDA-MB-231 human breast cancer cells. To rationalize the use of the animal model of MDA-MB-231 human breast cancer cells in this study, we first determined the presence of hypoxic regions in the bone metastases using a hypoxic marker pimonidazole. Immunohistochemical study showed the accumulation of pimonidazole in MDA-MB-231 cells colonized in bone (Fig. 1). Because pimonidazole accumulates in the cells that have oxygen concentration <10 mmHg pO_2, which corresponds to ~1.3% O_2 in the gas phase (2), the result suggests that the bone metastases in this animal model include equivalent levels of hypoxic regions to human breast cancers (4).

Effects of TOP3 on bone metastases of MDA-MB-231 cells. To study the role of hypoxia in bone metastases, we examined effects of TOP3 (12). Consistent with the previous report (12), our *in vitro* study using TAT-PTD-ODD-β-Gal showed that β-Gal activity was markedly increased in MDA-MB-231 cells cultured under the hypoxic condition compared with the cells cultured under normoxia, verifying the

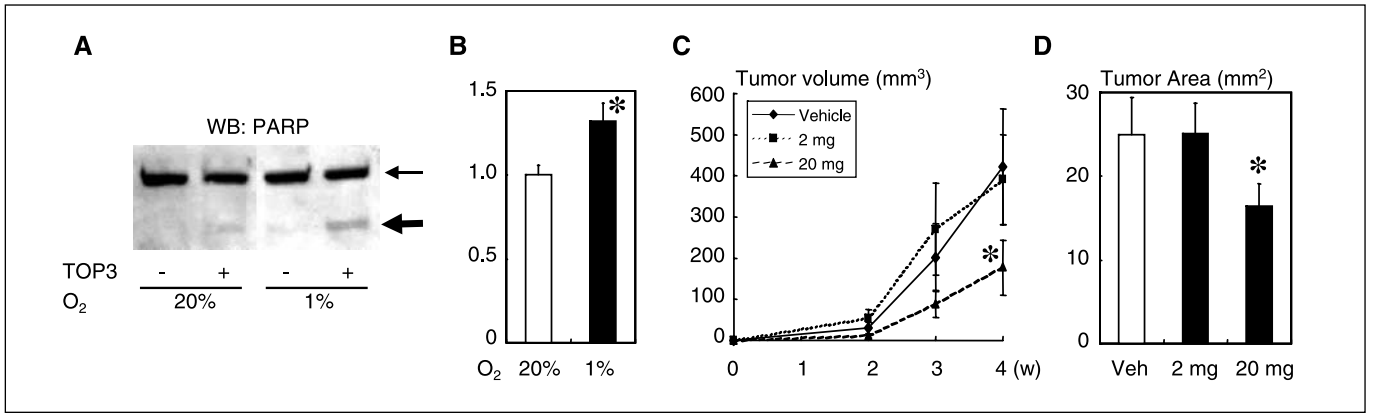

Figure 2. Effects of TOP3 on bone metastases of MDA-MB-231 cells. *A,* effect of TOP3 on the cleavage of PARP in MDA-MB-231 cells determined by Western blot (*WB*). The cells were cultured with TOP3 (15 μg/mL) for 36 h under 20% or 1% O_2 (*thin arrow,* intact PARP; *thick arrow,* cleaved PARP). *B,* effects of TOP3 on apoptosis in MDA-MB-231 cells. The cells were cultured with TOP3 (15 μg/mL) for 36 h under 20% or 1% O_2. Apoptosis was evaluated using FACS as described in Materials and Methods. Data are shown as apoptosis relative to 20% O_2. *C,* effects of TOP3 on the growth of MDA-MB-231 tumors in the orthotopic mammary fat pad. Data are shown as tumor volume (mm^3; *n* = 9/group). *, *P* < 0.05, significantly different from vehicle. *D,* effects of TOP3 on bone metastases of MDA-MB-231 cells. The metastatic tumor burden in bone was assessed by histomorphometry as described in Materials and Methods. Data are shown as tumor area (mm^2) / mouse (*n* = 9/group). *, *P* < 0.05, significantly different from vehicle.

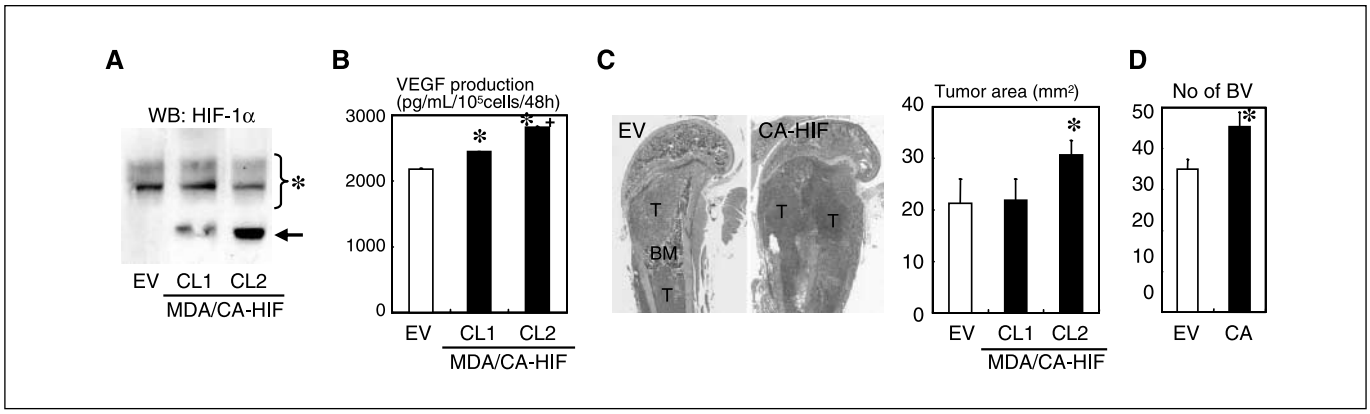

Figure 3. Effects of CA-HIF-1α on bone metastases of MDA-MB-231 cells. *A,* establishment of MDA-MB-231 cells overexpressing CA-HIF-1α (*MDA/CA-HIF*). Expression of CA-HIF-1α was determined by Western blot [*EV,* empty vector-transfected clone; clone 1 (*CL1*); low expression clone; clone 2 (*CL2*), high expression clone; *, endogenous wild-type HIF-1α; *arrow,* CA-HIF-1α]. *B,* VEGF production by MDA/CA-HIF. The cells were cultured with serum-free medium for 48 h under normoxia. The conditioned medium was collected and VEGF concentration was measured by ELISA. *Columns,* amount of VEGF produced (pg/mL/10^5 cells/48 h; n = 3/group). *, $P < 0.01$, significantly different from MDA/EV; +, $P < 0.01$, significantly different from MDA/CA-HIF clone 1. *C,* histomorphometric analysis of tumor burden of MDA/CA-HIF in the hind limbs in nude mice. *Left,* representative histologic view of bone metastases of MDA/EV (*EV*) and MDA/CA-HIF (clone 2; *CA-HIF*). H&E staining: *T*: tumor; *BM*: bone marrow, original magnification, ×25. Tumor burden was determined as described in Materials and Methods. Quantitative data are shown as tumor area (mm^2) / mouse (n = 9/group). *, $P < 0.05$, significantly different from MDA/EV. *D,* histomorphometric analysis of blood vessel density in bone metastases of MDA/CA-HIF (clone 2). Blood vessel density was determined as described in Materials and Methods. Data are shown as number of blood vessels (*BV*) / mm^2 tumor area (n = 9/group). *, $P < 0.05$, significantly different from MDA/EV.

oxygen-dependent stability of TAT-PTD-ODD fusion proteins in MDA-MB-231 cells (Supplementary Fig. S1). We then examined effects of TOP3 on MDA-MB-231 cells *in vitro*. Western blot analysis showed that TOP3 increased the cleavage of a caspase-3 substrate protein PARP in the hypoxic cultures (Fig. 2*A*). Furthermore, apoptosis in MDA-MB-231 cells was significantly increased by the TOP3 treatment under hypoxia (Fig. 2*B*). We further examined the effects of TOP3 on MDA-MB-231 tumors *in vivo*. I.p. administrations of TOP3 inhibited the orthotopic tumor formation and the development of bone metastases in a dose-dependent manner (Fig. 2*C* and *D*).

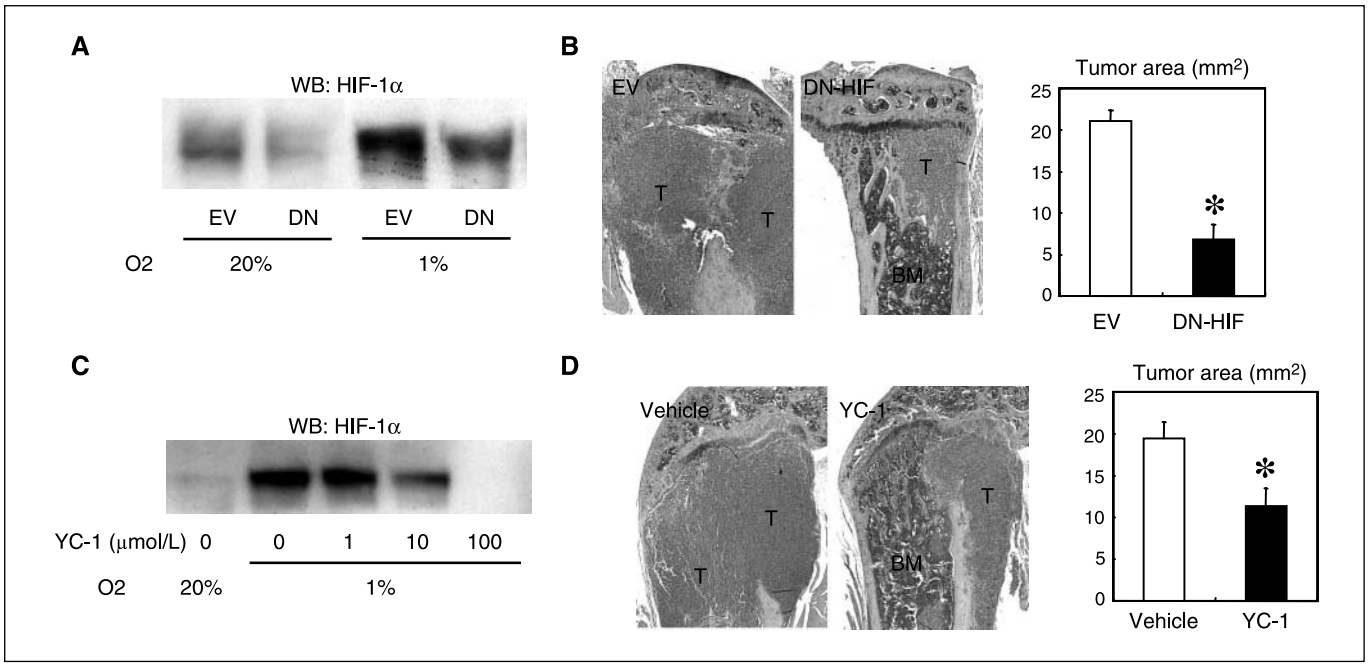

Figure 4. Effects of DN-HIF-1α and YC-1 on bone metastases of MDA-MB-231 cells. *A,* expression of endogenous wild-type HIF-1α in MDA/EV and MDA/DN-HIF (*DN*) under normoxia and hypoxia. *B,* histomorphometric analysis of tumor burden of MDA/DN-HIF in the hind limbs in nude mice. *Left,* representative histologic view of bone metastases of MDA/EV and MDA/DN-HIF (*DN-HIF*). H&E staining: *T*: tumor; *BM*: bone marrow, original magnification, ×25. Tumor burden was determined as described in Materials and Methods. Quantitative data are shown as tumor area (mm^2) / mouse (n = 9/group). *, $P < 0.05$, significantly different from MDA/EV. *C,* effects of YC-1 on nuclear HIF-1α expression in parental MDA-MB-231 cells. The cells were treated with YC-1 (1, 10, or 100 μmol/L) 5 min before being cultured under hypoxic conditions for 4 h. *D,* histomorphometric analysis of tumor burden of parental MDA-MB-231 cells in the hind limbs in nude mice treated without or with YC-1. *Left,* representative histologic view of bone metastases of parental MDA-MB-231 cells treated with vehicle or YC-1. H&E staining: original magnification, ×25. Tumor burden was determined as described in Materials and Methods. Quantitative data are shown as tumor area (mm^2) / mouse (n = 5/group). *, $P < 0.05$, significantly different from vehicle.

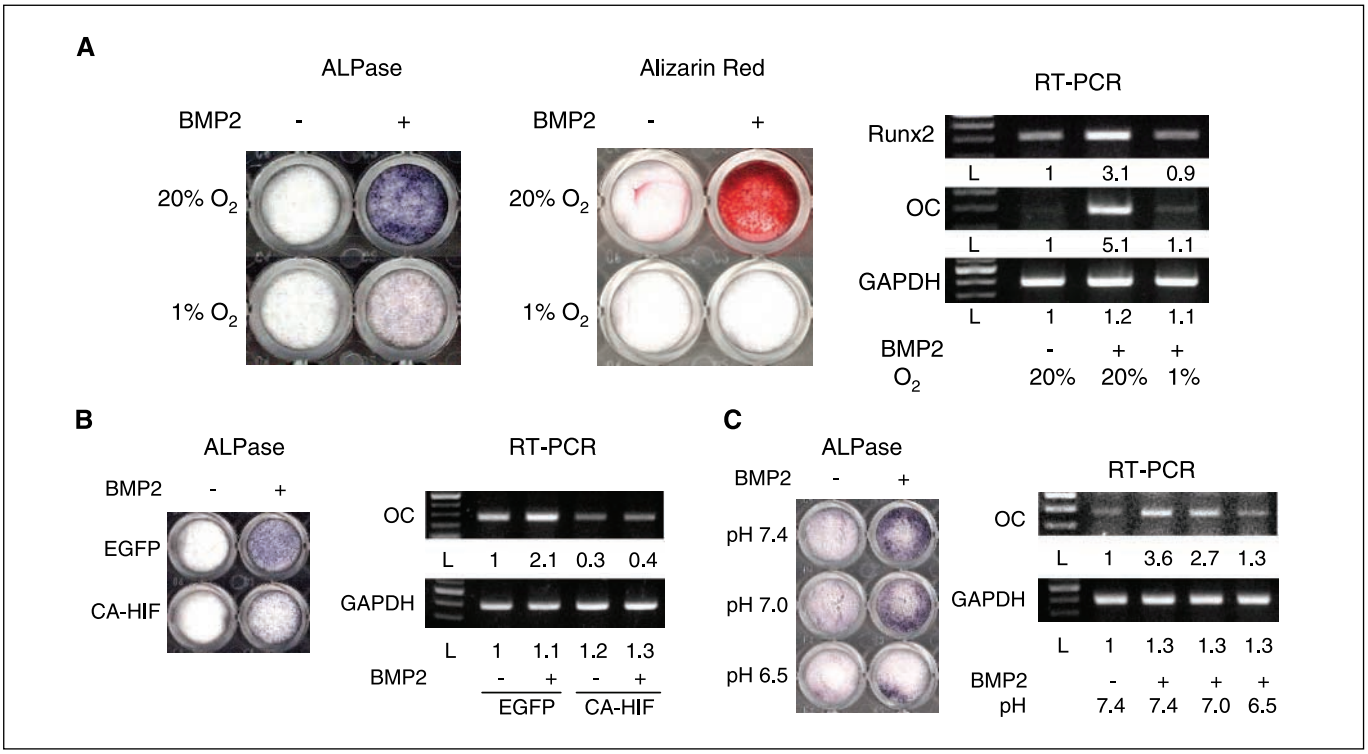

Figure 5. Effects of hypoxia, HIF-1 expression, and acidosis on osteoblast differentiation. *A,* effects of hypoxia on osteoblast differentiation determined by alkaline phosphatase (*ALPase*) activity in C3H10T1/2 cells, alizarin red staining of mouse primary calvarial osteoblasts, and semiquantitative RT-PCR analysis of *Runx2* and *osteocalcin* (*OC*) mRNA expression in C3H10T1/2 cells cultured with or without BMP2 (100 ng/mL) under normoxia or hypoxia. *B,* effects of HIF-1 expression on osteoblast differentiation determined by ALPase activity and *osteocalcin* mRNA expression in C3H10T1/2 cells infected with EGFP or CA-HIF-1α (*CA-HIF*) adenovirus. The cells were cultured with or without BMP2 (100 ng/mL) under normoxia. *C,* effects of acidosis on osteoblast differentiation determined by ALPase activity and *osteocalcin* mRNA expression in C3H10T1/2 cells cultured with the acidic medium in the presence or absence of BMP2 (100 ng/mL) under normoxia. Quantification of amplified mRNA was done as described in Materials and Methods and indicated as fold induction (*L,* 100 bp DNA ladder).

Effects of CA-HIF, DN-HIF, and YC-1 on bone metastases of MDA-MB-231. We then studied the role of HIF-1 in bone metastases. Western blot analysis showed that hypoxia induced HIF-1α accumulation in MDA-MB-231 cells *in vitro* (data not shown). Immunohistochemical study showed that the tumor cells with nuclear HIF-1α expression colocalized or surrounded the pimonidazole-positive cells in the bone metastases of MDA-MB-231 cells in nude mice (Fig. 1*C*). To examine the role of HIF-1 in bone metastases *in vivo*, we established MDA-MB-231 cells stably transfected with CA-HIF-1α cDNA (MDA/CA-HIF). Because CA-HIF-1α lacks the ODD domain (14), it is not degraded even under normoxic condition. Two clones of MDA/CA-HIF with low and high expression levels of CA-HIF-1α were used in the following experiments (Fig. 3*A*). ELISA showed that VEGF production was significantly increased in MDA/CA-HIF cells in a CA-HIF-1α expression–dependent manner (Fig. 3*B*). Radiological and histomorphometric analyses showed that osteolytic lesion area and tumor burden in bone were significantly increased in the high expression clone of MDA/CA-HIF (clone 2) compared with MDA/EV, whereas they were not changed in the low expression clone (clone 1; Fig. 3*C* and Supplementary Fig. S2). Blood vessel density determined by CD31 immunohistochemistry was significantly increased in the bone metastases of the MDA/CA-HIF (Fig. 3*D*).

To further determine the role of HIF-1 in bone metastases, we examined the capacity of MDA-MB-231 cells overexpressing DN-HIF-1α (MDA/DN-HIF; Supplementary Fig. S3) to develop bone metastases in nude mice. Western blot showed that nuclear HIF-1α accumulation was reduced in MDA/DN-HIF under both normoxic and hypoxic conditions (Fig. 4*A*). Histomorphometric examination showed that bone metastases were significantly reduced in MDA/DN-HIF (Fig. 4*B*). We also studied the effects of YC-1, which was shown to have inhibitory effects on the expression of HIF-1α and the induction of HIF-1 target genes, including *VEGF* (16), on bone metastases of MDA-MB-231 cells. YC-1 reduced nuclear HIF-1α expression also in MDA-MB-231 cells in a dose-dependent manner (Fig. 4*C*). Furthermore, YC-1 significantly decreased metastatic tumor burden of MDA-MB-231 cells in bone (Fig. 4*D*).

Effects of hypoxia and HIF-1 on bone cells. In bone metastases, bone cells, including osteoblasts, osteoclasts, and their precursor cells, share the common microenvironment with tumor cells colonized in bone. As shown in Supplementary Fig. S4, alkaline phosphatase–positive spindle-shaped osteoblast precursor cells and TRAP-positive mononuclear osteoclast precursor cells were adjacent to pimonidazole-positive hypoxic MDA-MB-231 cells, suggesting that hypoxia and HIF-1 activation may affect bone metabolism by influencing the differentiation of bone cells. Thus, we finally examined whether hypoxia and HIF-1 contribute to the induction of osteolysis frequently seen in bone metastases of breast cancer by studying their effects on osteoblasts and osteoclasts *in vitro*. The pluripotent mesenchymal cells C3H10T1/2 was shown to differentiate to alkaline phosphatase–positive osteoblast-like cells in the presence of BMP2 (17). Hypoxia markedly inhibited BMP2-induced alkaline phosphatase activity in C3H10T1/2 cells (Fig. 5*A*). BMP2-induced calcification in mouse primary osteoblasts determined by Alizarin red staining was also suppressed by hypoxia (Fig. 5*A*). Semiquantitative reverse transcription-PCR (RT-PCR)

analysis showed that hypoxia reduced BMP2-induced mRNA expression of the osteoblast differentiation markers, *Runx2* and *osteocalcin,* in C3H10T1/2 cells (Fig. 5*A*). Consistent with these results, the introduction of CA-HIF-1α by adenovirus inhibited BMP2-induced osteoblast differentiation and *osteocalcin* mRNA expression in C3H10T1/2 cells (Fig. 5*B*). In contrast, hypoxia increased TRAP-positive osteoclast-like cell formation in spleen cell cultures in the presence of sRANKL and M-CSF (Fig. 6*A*).

Hypoxia is frequently associated with low extracellular pH due to increased production of lactic acid through enhanced glycolysis (3). To approach the mechanisms of the suppressed differentiation of osteoblasts and the enhanced differentiation of osteoclasts under hypoxia, we examined the effects of acidosis on the differentiation of osteoblasts and osteoclasts. BMP2-induced alkaline phosphatase activity in C3H10T1/2 cells was reduced as the extracellular pH decreased (Fig. 5*C*). Acidic pH also suppressed BMP2-induced *osteocalcin* mRNA expression in C3H10T1/2 cells (Fig. 5*C*). In contrast, sRANKL and M-CSF–induced osteoclast differentiation in the spleen cell cultures was significantly increased in the low pH culture conditions (Fig. 6*B*).

Discussion

In solid tumors, oxygen delivery to tumor cells is frequently reduced by deteriorating diffusion geometry, severe structural abnormalities of microvessels, and disturbed microcirculation, leading to induce hypoxia. Previous reports using clinical samples showed that median tumor oxygen concentrations are generally lower than the surrounding normal tissues (1). Although the oxygen concentrations in bone metastases in cancer patients have not been explored yet, our immunohistochemical study using the hypoxic marker pimonidazole showed the presence of hypoxic regions in the bone metastases of MDA-MB-231 human breast cancer cells in nude mice. Because tissue oxygenation is associated with tumor size (2), our data that even relatively small size tumors in mouse bones include substantial hypoxic regions suggest that larger tumor mass in human bones likely have increased volume of hypoxic tumor cells. These results suggest that hypoxia may affect the pathophysiology of bone metastases of breast cancer.

To study the role of hypoxia in bone metastases, we tested the effects of TOP3 in our animal model. When used *in vivo*, the HIV-TAT fusion protein has been shown to be delivered to the entire body, including brain (13). The fusion protein is able to freely diffuse through cell membranes, and therefore through layers of tumor cells. Thus, HIV-TAT fusion proteins can be delivered to tissues where blood vessels are shut down, such as in ischemic brain (21). Consistent with the previous reports (12), our results showed that TOP3 was stabilized and caused caspase-3–induced apoptosis selectively in hypoxic MDA-MB-231 cells. Furthermore, animal experiments showed that the i.p. administration of TOP3 reduced the bone metastases as well as the orthotopic tumors of MDA-MB-231 cells. These results support the notion that hypoxia makes a substantial contribution to the development of bone metastases of breast cancer.

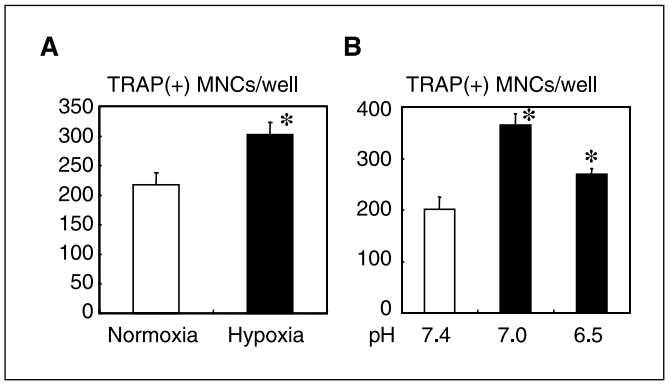

Figure 6. Effects of hypoxia and acidosis on osteoclast differentiation. Osteoclast-like cell formation was determined in spleen cell cultures in the presence of M-CSF (30 ng/mL) and sRANKL (50 ng/mL) under hypoxia (*A*) or acidic pH (*B*). Data are expressed as number of TRAP-positive multinucleated cells (*MNC*) per well per 48-well plate (n = 4/group). *, $P < 0.05$, significantly different from normoxia or pH 7.4.

Hypoxia causes a variety of biological responses in tumor cells. The transcription factor HIF-1 is a master mediator of the hypoxic response of tumor cells and controls the up-regulation of a number of factors vital for tumor expansion, including angiogenic factors such as VEGF. Western blot analysis showed that hypoxia induced HIF-1α accumulation in MDA-MB-231 cells and immunohistochemical study revealed the hypoxia-associated nuclear HIF-1α expression in MDA-MB-231 cells colonized in bone. The localization of the HIF-1α–positive cells and the pimonidazole-incorporated cells was not identical (Fig. 1). However, according to the recent report by Sobhanifer et al. (22), HIF-1α expression is decreased in perinecrotic regions of solid tumors. In addition, pimonidazole accumulates in the cells only below 1.3% O_2. These may account for the discrepancy.

The overexpression of CA-HIF-1α in MDA-MB-231 cells increased the production of one of the HIF-1 target gene product VEGF. Furthermore, CA-HIF-1α enhanced the progression of bone metastases of MDA-MB-231 cells accompanied with the increased number of CD31-positive microvessels. It is well known that angiogenesis is critical to tumor growth, survival, and metastasis (23). The previous reports showed that the inhibitors of angiogenesis reduced bone metastases in animal models (24, 25). These results collectively suggest that the promoted angiogenesis by the elevated VEGF production might play a causative role in the increased tumor burden in MDA/CA-HIF.

Breast cancer frequently causes osteolysis in bone metastases (11). Osteolysis in bone metastasis is thought to be due to the uncoupling between osteoclastic bone resorption and osteoblastic bone formation. It is widely recognized that osteolysis is caused by the production of osteoclast-activating factors such as parathyroid hormone-related protein (11). In addition, recent studies showed that the Wnt signal inhibitors, dickkopf-1 and secreted Frizzled-related protein-2, also play roles in the development of osteolytic lesions in multiple myeloma by inhibiting bone formation (26, 27). Consistent with the previous reports (28, 29), our results showed that hypoxia inhibited osteoblast differentiation of the multipotent mesenchymal cells C3H10T1/2 and mouse primary calvarial osteoblasts *in vitro*. In addition, we showed that the introduction of CA-HIF-1α inhibited osteoblast differentiation of C3H10T1/2 cells, suggesting that hypoxia-induced inhibition of osteoblast differentiation is, at least in part, dependent on HIF-1. We also found that acidosis, which is frequently caused by hypoxia, has a negative effect on osteoblast differentiation as well as osteoblast function (30, 31). The result suggests that hypoxia-induced acidic microenvironment contributes to the inhibition of osteoblast differentiation. In contrast to the effects on osteoblast differentiation, hypoxia stimulated osteoclast-like cell formation in mouse spleen cell culture. Arnett et al. (32) and Fukuoka et al. (33) showed

similar results. Furthermore, acidosis also enhanced osteoclast differentiation in a pH-dependent manner. As the molecular mechanisms of the acidosis-increased osteoclast formation, Frick et al. (34) reported that metabolic acidosis stimulates mRNA expression of *RANKL* in bone cells. Komarova et al. (35) showed that acidosis directly acts on osteoclasts to activate nuclear factor of activated T cells c1, the critical transcription factor to osteoclast differentiation (36). These results collectively suggest that hypoxia and HIF-1 are involved in the formation of osteolytic bone metastases by suppressing osteoblast differentiation and stimulating osteoclast differentiation.

Bone metastasis is often classified as either osteolytic or osteoblastic. Osteoblastic metastases are frequently seen in prostate cancer patients. However, oxygen levels in prostate cancer are comparable or even lower than that in breast cancer (37, 38). Osteoblastic metastasis is believed to be caused by the cancer cell production of factors that stimulate osteoblast proliferation, differentiation, and bone formation. Several lines of experimental evidence have shown that prostate cancer cells promote osteoblastic activity by secreting osteoblast-stimulating factors, including BMPs (39, 40). These results suggest that, in the bone metastases of prostate cancer, these osteoblastic factors may play a dominant role in the formation of osteoblastic metastases even in the hypoxic condition.

In conclusion, the results suggest that tumor-associated hypoxia and HIF-1 expression promote the progression of bone metastases in breast cancer. Our results also suggest that hypoxia and HIF-1 also play a role in the induction of osteolytic change in bone metastases through causing an uncoupling between bone resorption and formation. Hypoxia and HIF-1 may be potential therapeutic targets for bone metastases in breast cancer.

Acknowledgments

Received 6/28/2006; revised 1/11/2007; accepted 2/12/2007.

Grant support: Grants in aid 14771020, 16791123, 18592031 (T. Hiraga), 17014058 and 21st century Center of Excellence program (T. Yoneda) from the Ministry of Education, Culture, Sports, Science and Technology, Japan; Senri Life Science Foundation Research Grant (T. Hiraga); Osaka Cancer Society Research Grant (T. Hiraga); and Research Grant from Sagawa Foundation for Promotion of Cancer Research (T. Hiraga).

The costs of publication of this article were defrayed in part by the payment of page charges. This article must therefore be hereby marked *advertisement* in accordance with 18 U.S.C. Section 1734 solely to indicate this fact.

References

1. Brown JM, Wilson WR. Exploiting tumor hypoxia in cancer treatment. Nat Rev Cancer 2004;4:437–47.
2. Kizaka-Kondoh S, Inoue M, Harada H, Hiraoka M. Tumor hypoxia: a target for selective cancer therapy. Cancer Sci 2003;94:1021–8.
3. Harris AL. Hypoxia—a key regulatory factor in tumor growth. Nat Rev Cancer 2002;2:38–47.
4. Vaupel S, Briest S, Hockel M. Hypoxia in breast cancer: pathogenesis, characterization and biological/therapeutic implications. Wien Med Wochenschr 2002;152:334–42.
5. Semenza GL. Targeting HIF-1 for cancer therapy. Nat Rev Cancer 2003;3:721–32.
6. Huang LE, Bunn HF. Hypoxia-inducible factor and its biomedical relevance. J Biol Chem 2003;278:19575–8.
7. Bos R, Zhong H, Hanrahan CF, et al. Levels of hypoxia-inducible factor-1α during breast carcinogenesis. J Natl Cancer Inst 2001;93:309–14.
8. Zhong H, De Marzo AM, Laughner E, et al. Overexpression of hypoxia-inducible factor 1α in common human cancers and their metastases. Cancer Res 1999;59:5830–5.
9. Gruber G, Greiner RH, Hlushchuk R, et al. Hypoxia-inducible factor 1α in high-risk breast cancer: an independent prognostic parameter? Breast Cancer Res 2004;6:R191–8.
10. Schindl M, Schoppmann SF, Samonigg H, et al. Overexpression of hypoxia-inducible factor 1α is associated with and unfavorable prognosis in lymph node-positive breast cancer. Clin Cancer Res 2002;8:1831–7.
11. Mundy GR. Metastasis to bone: causes, consequences and therapeutic opportunities. Nat Rev Cancer 2002;2:584–93.
12. Harada H, Hiraoka M, Kizaka-Kondoh S. Antitumor effect of TAT-oxygen-dependent degradation-caspase-3 fusion protein specifically stabilized and activated in hypoxic tumor cells. Cancer Res 2002;62:2013–8.
13. Schwarze SR, Ho A, Vocero-Akbani A, Dowdy SF. *In vivo* protein transduction: delivery of a biologically active protein into the mouse. Science 1999;285:1569–72.
14. Kelly BD, Hackett SF, Hirota K, et al. Cell type-specific regulation of angiogenic growth factor gene expression and induction of angiogenesis in nonischemic tissue by a constitutively active form of hypoxia-inducible factor 1. Circ Res 2003;93:1074–81.
15. Kasuno K, Takabuchi S, Fukuda K, et al. Nitric oxide induces hypoxia-inducible factor 1 activation that is dependent on MAPK and phosphatidylinositol 3-kinase signaling. J Biol Chem 2004;279:2550–8.
16. Yeo E-J, Chun Y-S, Cho Y-S, et al. YC-1: a potential anticancer drug targeting hypoxia-inducible factor 1. J Natl Cancer Inst 2003;95:516–25.
17. Ichida F, Nishimura R, Hata K, et al. Reciprocal roles of Msx2 in regulation of osteoblast and adipocyte differentiation. J Biol Chem 2004;279:34015–22.
18. Hiraga T, Myoui A, Choi ME, Yoshikawa H, Yoneda T. Stimulation of cyclooxygenase-2 expression by bone-derived transforming growth factor β enhances bone metastases in breast cancer. Cancer Res 2006;66:2067–73.
19. Ito M, Amizuka N, Tanaka S, et al. Ultrastructural and cytobiological studies on possible interactions between PTHrP-secreting tumor cells, stromal cells, and bone cells. J Bone Miner Metab 2003;21:353–62.
20. Miyake S, Makimura M, Kanegae Y, et al. Efficient generation of recombinant adenoviruses using adenovirus DNA-terminal protein complex and a cosmid bearing the full-length virus genome. Proc Natl Acad Sci U S A 1996;93:1320–4.
21. Asoh S, Ohsawa I, Mori T, et al. Protection against ischemic brain injury by protein therapeutics. Proc Natl Acad Sci U S A 2002;99:17107–12.
22. Sobhanifar S, Aquino-Parsons C, Stanbridge EJ, Olive P. Reduced expression of hypoxia-inducible factor-1a in perinecrotic regions of solid tumors. Cancer Res 2005;65:7259–66.
23. Ferrara N, Kerbel RS. Angiogenesis as a therapeutic target. Nature 2005;438:967–74.
24. Sasaki A, Alcalde RE, Nishiyama A, et al. Angiogenesis inhibitor TNP-470 inhibits human breast cancer osteolytic bone metastasis in nude mice through the reduction of bone resorption. Cancer Res 1998;58:462–7.
25. Weber MH, Lee J, Orr FW. The effects of Neovastat (AE-941) on an experimental metastatic bone tumor model. Int J Oncol 2002;20:299–303.
26. Tian E, Zhan F, Walker R, et al. The role of the Wnt-signaling antagonist DKK1 in the development of osteolytic lesions in multiple myeloma. N Engl J Med 2003;349:2483–94.
27. Oshima T, Abe M, Asano J, et al. Myeloma cells suppress bone formation by secreting a soluble Wnt inhibitor, sFRP-2. Blood 2005;106:3160–5.
28. Park JH, Park BH, Kim HK, Park TS, Baek HS. Hypoxia decreases Runx2/Cbfa1 expression in human osteoblast-like cells. Mol Cell Endocrinol 2002;192:197–203.
29. Salim A, Nacamuli RP, Morgan EF, Giaccia AJ, Longaker MT. Transient changes in oxygen tension inhibit osteogenic differentiation and Runx2 expression in osteoblasts. J Biol Chem 2004;279:40007–16.
30. Tuncay OC, Ho D, Barker MK. Oxygen tension regulates osteoblast function. Am J Orthod Dentofacial Orthop 1994;105:457–63.
31. Warren SM, Steinbrech DS, Mehrara BJ, et al. Hypoxia regulates osteoblast gene expression. J Surg Res 2001;99:147–55.
32. Arnett TR, Gibbons DC, Utting JC, et al. Hypoxia is a major stimulator of osteoclast formation and bone resorption. J Cell Physiol 2003;196:2–8.
33. Fukuoka H, Aoyama M, Miyazawa K, Asai K, Goto S. Hypoxic stress enhances osteoclast differentiation via increasing IGF2 production by non-osteoclastic cells. Biochem Biophys Res Commun 2005;328:885–94.
34. Frick KK, Bushinsky DA. Metabolic acidosis stimulates RANKL RNA expression in bone through a cyclo-oxygenase-dependent mechanism. J Bone Miner Res 2003;18:1317–25.
35. Komarova SV, Pereverzev A, Shum JW, Sims SM, Dixon SJ. Convergent signaling by acidosis and receptor activator of NF-κB ligand (RANKL) on the calcium/calcineurin/NFAT pathway in osteoclasts. Proc Natl Acad Sci U S A 2005;102:2643–8.
36. Takayanagi H, Kim S, Koga T, et al. Induction and activation of the transcription factor NFATc1 (NFAT2) integrate RANKL signaling in terminal differentiation of osteoclasts. Dev Cell 2002;3:889–901.
37. Movsas B, Chapman JD, Greenberg RE, et al. Increasing levels of hypoxia in prostate carcinoma correlate significantly with increasing clinical stage and patient age: an Eppendorf pO_2 study. Cancer 2000;89:2018–24.
38. Movsas B, Chapman JD, Hanlon AL, et al. Hypoxia in human prostate carcinoma: an Eppendorf pO_2 study. Am J Clin Oncol 2001;24:458–61.
39. Dai J, Keller J, Zhang J, Lu Y, Yao Z, Keller ET. Bone morphogenetic protein-6 promotes osteoblastic prostate cancer bone metastases through a dual mechanism. Cancer Res 2005;65:8274–85.
40. Masuda H, Fukabori Y, Nakano K, Takezawa Y, Suzuki T, Yamanaka H. Increased expression of bone morphogenetic protein-7 in bone metastatic prostate cancer. Prostate 2003;54:268–74.